





Stochastic superflares of photoluminescence from a single microdiamond with germanium-vacancy color centers: A general phenomenon or a unique observation

Natalia A. Lozing ^{1,2,3} Maxim G. Gladush ^{1,3} Ivan Yu. Eremchev ^{1,3} Eugeniy A. Ekimov,⁴ and Andrey V. Naumov ^{1,3,*}

¹*Institute for Spectroscopy of the Russian Academy of Sciences, 5 Fizicheskaya Street, Troitsk, 108840 Moscow, Russia*

²*National Research University Higher School of Economics, 20 Myasnitskaya Street, 101000 Moscow, Russia*

³*Moscow State Pedagogical University, 1/1 M. Pirogovskaya Street, 119991 Moscow, Russia*

⁴*Vereshchagin Institute for High Pressure Physics of the Russian Academy of Sciences, Troitsk, 108840 Moscow, Russia*



(Received 20 October 2019; accepted 29 June 2020; published 12 August 2020)

We report the discovery of a GeV-associated phenomenon which is strong (up to an order) stochastic reversible enhancements of photoluminescence intensity in a single GeV diamond synthesized with the high-pressure, high-temperature technique. We were lucky to observe this effect with only one crystal among dozens of similar microdiamonds. Each rise and fall of the intensity above its stable moderate level may be referred to as a superflare with smooth dynamics of the transients which develop on the timescale of seconds. These flares tend to recur infinitely at ambient conditions under cw-laser excitation above a certain input power threshold. To explain this phenomenon we propose a theory of intrinsic optical instabilities which develop in a dense ensemble of quantum emitters.

DOI: [10.1103/PhysRevB.102.060301](https://doi.org/10.1103/PhysRevB.102.060301)

Photoluminescence from individual emitters and ensembles can be very different in their properties and applications. It is noteworthy that the ensemble radiation may be not just a collection of light from several separate sources. It is known that ensemble photoluminescence can produce coherent light, have more than one steady state, and show long transients or dynamic chaos if certain conditions are met [1]. The class of luminescent materials which has been proven to demonstrate both single source [2] and ensemble emission [3] is diamonds with different atom-vacancy defects known as diamond color centers. They are used in a lot of applications including luminescent markers [4], magnetic field sensing [5], single-photon sources for quantum cryptography and information processing [6], temperature sensors [7], and others [8]. The nitrogen-vacancy (NV) center is the most well-studied color center in diamond [2], but it has a few important disadvantages such as a broad emission spectrum dominated by the phonon sideband (PSB). Among the recent trends significant efforts have been put into the fabrication and studying of silicon-vacancy (SiV) [9,10] and germanium-vacancy (GeV) [9,11] centers. Due to the symmetrical structure, the SiV center has a narrow inhomogeneous linewidth and is reported to demonstrate spectral and emission stabilities. GeV centers have a similar structure and are likely to rival the excellent optical properties of SiV diamonds. The GeV diamonds are relatively new materials and are fabricated using high-pressure, high-temperature (HPHT) synthesis [12], chemical vapor deposition (CVD), and ion implantation [6] that provide

diamonds of various forms and sizes. In all fabrication variants GeV photoluminescence demonstrates the narrow zero-phonon line (ZPL) emission at 602.5 nm with a full width at half maximum of 4–5 nm at room temperature [6,12].

In this Rapid Communication we describe our studies of spectral properties of a few dozens of single HPHT diamond microcrystals with GeV⁻ centers. Surprisingly, one of the crystals was discovered to show a very unusual fluorescent behavior, which is our main concern. This specific microcrystal showed no differences from all the others in either the complex spectroscopic studies (including the widefield and confocal fluorescence microscopy techniques) or in the atomic force microscopy (AFM) images [see Supplemental Material (SM) [13]].

The photoluminescence intensity of single microcrystals under cw-laser excitation was measured as a function of time using an epiluminescence microscope (for the experimental details and sample preparation technique, see the SM [13] and in [14–17]). The microcrystals were identified by the presence of the characteristic ZPL in the photoluminescence (PL) emission spectrum near 602 nm and in the photoluminescence excitation (PLE) spectrum. The sizes of single crystals were measured by an AFM and were shown to vary from hundreds of nanometers to several micrometers. The right and middle insets in Fig. 1 show the surface profiles of the sample containing three objects, two of which are the diamonds with GeV centers, marked as “T” (typical) and “N” (nontypical) (with characteristic dimensions of 600 nm and 2 μm, correspondingly). All the objects were separated by a distance of about 5 μm, which made it possible to obtain the nonoverlapping fluorescent images (see the left-hand side inset) and to extract fluorescence data from each object simultaneously. Figure 1 shows fluorescence intensity trajectories from the “T” and “N”

*Corresponding author: a_v_naumov@mail.ru,
www.single-molecule.ru

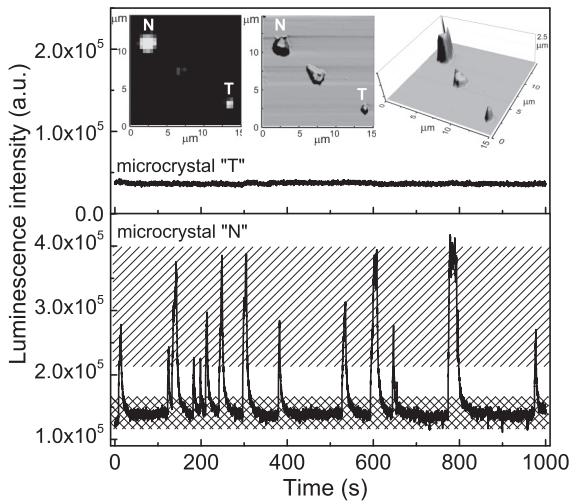


FIG. 1. Typical (upper) and nontypical (bottom) PL intensity trajectories from GeV microcrystals marked as “N” and “T,” correspondingly. Excitation wavelength is 602 nm. Insets: fluorescent image (left) and AFM images (center and right). The levels shaded by diagonal-line and crossed-line patterns correspond accordingly to the bright and the dim states.

samples measured simultaneously in one experimental run. One may see that the fluorescence intensity from “T” (upper track in Fig. 1) has relatively small fluctuations and remains stable during the entire observation. The same behavior was observed for all the other microcrystals except for crystal “N” (bottom track in Fig. 1). The emission from “N” was seen to increase at random instants of time and return back to the well-designated level. Both transitions demonstrated well-pronounced profiles of long-time dynamics. We will refer to the low-level and high-level emission intensities as “dim” and “enhanced” states, correspondingly. The excitation power dependencies are shown in Fig. 2. The dim states vs power are denoted by stars and demonstrate linear growth with negligible variations at each fixed excitation (see the guidance shading). In contrast, the enhanced states (denoted by circles) show large spreads of intensities marked by the shaded region. The existence of this spread complicates the power dependence analysis: the data can be equally well fitted by either a linear or a nonlinear function with saturationlike behavior (see the dashed guideline in Fig. 2). However, it is

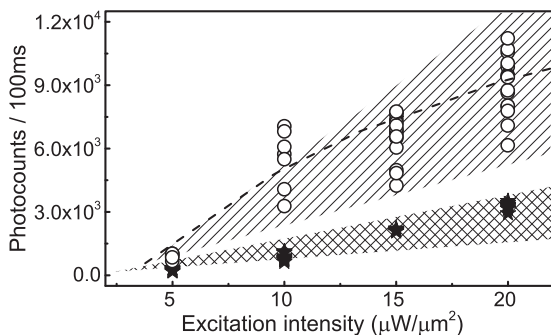


FIG. 2. Dim (stars) and bright (circles) intensity variations versus incident power.

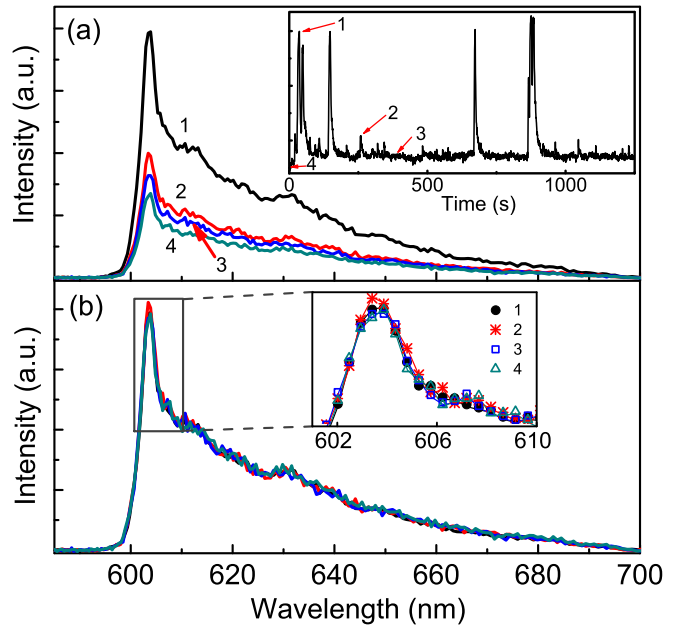


FIG. 3. (a) PL spectra from microcrystal “N” in different emission states. The inset shows the emission trail with numbered time moments for PL curves. (b) PL spectra as in (a) scaled correspondingly to the peak intensity ratio. Excitation wavelength is 590 nm; excitation intensity is $18 \mu\text{W}/\mu\text{m}^2$.

evident that in both cases the slopes of the fitting functions for the enhanced states must be notably steeper than those for the dim intensities. In addition, there is a splitting point near the first excitation power that was proved to be a threshold for the existence of the enhanced intensity states. These facts, in principle, may serve as clues to the enhancement mechanism which we discuss further.

Figure 3(a) shows PL spectra for “N” in different emission states, where one can see well-resolved narrow ZPLs around 602 nm with broad PSBs (for PLE spectra, see the SM [13]). The inset illustrates the fragment of the fluorescent track with the numbered time moments which correspond to the numbered spectra. To investigate possible changes in the ZPL and PSB shapes we normalized the contours and found no noticeable differences between the enhanced and dim spectral parameters including ZPL linewidth [see Fig. 3(b) and inset]. This result means that the enhanced emission is not likely to occur due to the stochastic switching to the amplified spontaneous emission regime or random lasing. Any lasing is usually expected to be marked by narrowing of the emission spectra; however, this evidently is not our case. Note that there is some asymmetry in the durations of the transitions, i.e., the dim-to-enhanced is generally shorter than the enhanced-to-dim transient (Fig. 4), but with high input powers the enhanced-to-dim transitions tend to develop faster. The intensity decay curves are best fitted by the biexponential time function with characteristic time constants t_1 from 0.3 to 4.7 s and t_2 from 1.5 to 38 s, where for higher powers both tend to decrease (see the SM [13]). As for the dim-to-enhanced transitions, the characteristic times are hard to be recovered because of the complex slope shapes. However, the trend may be roughly estimated to be about 3 and 1 s for low and high input powers,

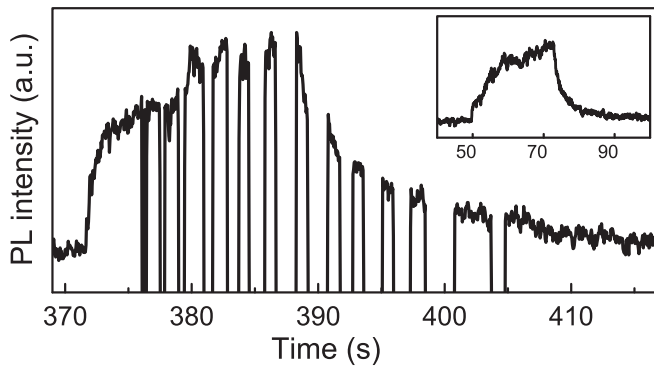


FIG. 4. Temporal evolution of PL intensity during a single superflare with periodic shattering of cw excitation. The inset shows a similar single superflare observed without shattering of excitation for this crystal at a different experimental run.

respectively. In addition, the number of transitions per time interval grows with power while the duration of the enhanced emission tends to decrease from a few dozens of seconds to seconds. Multiple variants of the transients and the steady states may be found in the SM [13].

Another remarkable observation was to show crystal “N” return exactly to its current emission state after a short (1–2 s) interruption of the pump as shown in Fig. 4. After resuming the input the fluorescence restores itself quickly to almost the same level and proceeds with the enhanced-to-dim process. The inset in Fig. 4 shows the example of emission trail without interruptions.

The stochastic switching between dark and bright PL states (including intermediate gray states) is a very well-known phenomenon referred to as blinking. It has been observed with different types of nanoemitters including organic dye molecules and molecular complexes [18], quantum dots [19], perovskite particles [20], and, also, with the single color centers in diamonds [21]. In general, the physical (microscopic) origin of blinking is a specific case for each system. In most cases blinking is observed for PL of single quantum emitters and explained by the existence of single or multiple channels of nonradiative relaxation of the excited state of the emitter. In some cases (single molecules at cryogenic temperatures, NV centers) it is the result of the variation of absorption spectra. For example, the blinking observed in NV centers in diamonds was explained as the charge dynamics of single NV centers [21]. The latter is obviously not applicable to our case. In fact, it is evident that the number of emitting GeV centers in the microcrystal under study is greater than just a few. The parameters of HPHT synthesis allow the estimates of this number to be as high as a hundred or more. It corresponds to the number density of the emitters greater than 10^{14} cm^{-3} . Moreover, PL blinking has intervals with sharp boundaries, i.e., the switching time is much shorter than the exposure time. It is the key point in distinguishing this type of PL intensity fluctuations from our case. Thus, together with the long-lasting transients, we believe that some cooperative effects are responsible as they require some time for the multiple cross interactions to have worked producing a steady state. While only one from the dozens of microcrystals observed demonstrated this superflare effect, at this stage of

the investigation we can only propose this model, but do not claim that this model is the only possibility.

Hypothetically, collective charge modifications of GeV centers in an ensemble could be arising from a volume charge diffusion that can change the PL intensity. However, even beyond the discussion about the origin of such diffusion, there is no explanation of the existence of an excitation power threshold for the superflares to start. The threshold seen in Fig. 2 indicates a photoinduced effect which is hard to explain both for a single center and for an ensemble of independent emitters.

The long-range (second and subsecond scale) dynamics of the PL intensity flares were reported recently in, for instance, perovskite microcrystals [22] and CaS:Eu crystals [23], but the time patterns were rather distinct from our observations. In addition, the key feature in our experiment was the prevailing in the time-constant dim steady state (sawlike time patterns vs our rare flares).

Instabilities with lengthy transients could be signatures of collective behavior in a many-particle system. In this regard, we consider the optical bi- (OB) and multistability (OM). These are the situations when ensembles of emitters realize two or more emission steady states overlapping for certain ranges of the input power with a possibility to switch between them. Such instabilities may develop if the conditions provide optical feedback and nonlinearities in the system’s response to the incident light. OB and OM can be caused by either extrinsic [24] or intrinsic [25] feedback mechanisms. Once such a system comes to a steady emission some disturbances in the system parameters may arise and force it to switch to another steady state after having gone through a finite-time transient process. Both cases are known to have transient dynamics when going from one stable state to another [26,27] with lengthy transient phases [28–30]. The observations of OB and OM have been supported by various theories that utilize the two-level and multilevel atomlike schemes to describe the emitters. A recent article has proposed a theory for the four-level GeV diamond scheme to simulate OB and OM in a ring cavity [31]. It was shown that the instabilities were very sensitive to the parameters which include the detunings of probe and coupling fields, the powers of the coupling fields, and the density of GeV centers. The OB thresholds, as well as switchings between OB and OM regimes, were described as controllable via changing these parameters.

Since in our system there is no external feedback like in [31] we address the intrinsic optical bistability (IOB) or multistability (IOM). In these cases the positive feedback is intrinsic and is provided by the secondary field generated by the emitters as a part of some complex collective response to external excitation. In the systems of emitters in solid hosts experimental observations of IOB have been reported in a few papers (e.g., see the early paper [25]). The state-of-the-art theoretical developments of IOB/IOM are described in [32], and the references therein. However, in our analysis we will expand the original theory from [33,34] for a collection of quantum emitters distributed in a continuous host material that by itself (e.g., diamond lattice) is weakly absorptive towards the incident light. The density matrix ρ of a single emitter from such an ensemble is to be found from the equation which in its general form [33] in the interaction picture and the

electric dipole approximation may be written as

$$i \frac{d}{dt} \rho = -\frac{\hat{l}(\varepsilon)}{\hbar} \left[\hat{\mathbf{d}} \left(\mathbf{E} + \int_0^t dt' \sum_{e' \neq e} G_{ee'} \mathbf{p}_{e'} \right), \rho \right] - \frac{\hat{l}(\varepsilon)}{\hbar} \left[\hat{\mathbf{d}}, \int_0^t dt' (G_{ee}^+ \rho \hat{\mathbf{d}} + G_{ee}^- \hat{\mathbf{d}} \rho) \right], \quad (1)$$

where $\hat{\mathbf{d}} = \hat{\mathbf{d}}(t)$ is the dipole transition operator, $\mathbf{E} = \mathbf{E}(\mathbf{r}_e, t)$ is the macroscopic field in the host at the position of the emitter \mathbf{r}_e , $G_{ee'} = G(\mathbf{r}_e - \mathbf{r}_{e'}, t - t')$ is the Green's tensor for the field inside the host with \pm superscripts indicating the tensor's advanced and retarded components respectively, vectors $\mathbf{p}_{e'} = \mathbf{p}_{e'}(t') = \text{Tr}(\rho_{e'} \hat{\mathbf{d}}_{e'})$ are induced dipoles of the emitters at positions $\mathbf{r}_{e'}$, and $\hat{l}(\varepsilon)$ is a local-field correction produced by the host with complex permittivity $\varepsilon = \varepsilon(\omega_0)$ at the frequency ω_0 of the external field. The other notations are conventional and refer accordingly to time, the imaginary unit, the reduced Plank constant, and the commutator. In this equation the first commutator describes coupling of the target emitter to the mean field that consists of the medium-modified external fields and the response from the other emitters all corrected with the factor describing the averaged response from the host. In ensembles with moderate inhomogeneities these fields may produce sufficient feedback to give rise to IOB (IOM). The second commutator is the local-field enhanced radiative decay. An explicit form of $\hat{\mathbf{d}}$ and a particular composition of \mathbf{E} would bring Eq. (1) to one of the ‘‘atom-field’’ interaction schemes. In this work we describe the two-level model with states ‘‘1’’ and ‘‘2’’ and transition frequency ω_e to give a qualitative description of the experiment.

Equation (1) can be transformed to the solvable form $id\rho/dt = 1/\hbar[\hat{H}^{rw}, \rho] + i\hat{R}(\rho)$ by applying the Born-Markov approximation, transforming to the Schrödinger picture, and changing to the rotating frame with matrix ρ . Here, \hat{H}^{rw} is the Hamiltonian with the effective detuning Δ and the effective Rabi frequency $\Omega = \Omega(\rho)$ that provides the feedback. The operator $\hat{R}(\rho) = \gamma/2\hat{L}_{\sigma^-}(\rho) + \gamma_{\perp}\hat{D}(\rho)$ describes, respectively, the radiative relaxation via the Lindblad operator $\hat{L}_{\hat{\rho}}(\rho) = 2\hat{\rho}\hat{\rho}^{\dagger} - \hat{\rho}^{\dagger}\hat{\rho}\rho - \rho\hat{\rho}^{\dagger}\hat{\rho}$ and dephasing with $\hat{D}(\rho) = 2\hat{\sigma}_z\hat{\rho}\hat{\sigma}_z - \hat{\sigma}_z\hat{\rho}\hat{\sigma}_z - \rho\hat{\sigma}_z\hat{\sigma}_z$, where $\hat{\sigma}_{\pm}$ and $\hat{\sigma}_z$ are atomic projection operators and γ and γ_{\perp} are the effective longitudinal and transverse rates. Note that the dephasing term does not follow from Eq. (1) but could be derived as in [33,34]. We may rewrite ρ in the Bloch vector basis as $\rho = 1/2(\hat{\mathbf{I}} + \mathbf{B} \cdot \boldsymbol{\sigma})$, where $\hat{\mathbf{I}}$ is a unit matrix, $\mathbf{B}^T = \{\varrho_{21} + \varrho_{12}, i(\varrho_{12} - \varrho_{21}), \varrho_{11} - \varrho_{22}\} = \{u, v, w\}$ is the Bloch vector with matrix elements ϱ_{ij} , and $\boldsymbol{\sigma}$ is a vector with the Pauli matrices as components. Resolving the master equation with respect to the population difference w in the steady state we get the polynomial (see the SM [13])

$$\eta^2 w^3 - (\eta^2 + \zeta^2) w^2 + (\zeta^2 + \Delta^2 + \Gamma^2 + \beta^2) w - (\Delta^2 + \Gamma^2) = 0, \quad (2)$$

which depending on parameters has either a single real number root w or three linking solutions w_1, w_2 , and w_3 producing a bistability region. Parameters $\eta^2 = |\varepsilon|^2 \xi^2$ and $\zeta^2 = (2\varepsilon_R \Delta - \varepsilon_I \Gamma) \xi$ contain the cooperativity factor $\xi = \xi(N_e)$ which arises from the ensemble local field and, thus, is a

function of either the density N_e or the absolute number of the emitters. The host contributes a complex-number factor $\varepsilon = l(\varepsilon)/\varepsilon = \varepsilon_R + i\varepsilon_I$. Physically η^2 represents a squared renormalized ξ while ζ^2 is a cross term of ξ with Δ and the effective decay rate Γ . The latter are $\Delta = (\omega_e - \omega_0) - \delta$ and $\Gamma = \gamma_{\perp} + \gamma$, where $\delta = [l_R - (\kappa l_R + n l_I) \gamma_0 / (2\delta_0)] \delta_0$ is the effective radiative frequency shift and $\gamma = [n l_R - (\kappa - 2\delta_0 / \gamma_0) l_I] \gamma_0$. These expressions must be understood as corrections to the natural values $\delta_0 = (1/\hbar) \text{Re}[\mathbf{d} \cdot \mathbf{G}_{ee}^0(\omega_e) \cdot \mathbf{d}]$ and $\gamma_0 = (2/\hbar) \text{Im}[\mathbf{d} \cdot \mathbf{G}_{ee}^0(\omega_e) \cdot \mathbf{d}]$ where the Green's tensor is written for vacuum. The local field from the host gives the factors $l(\varepsilon) = l_R + i l_I$ and also $\sqrt{\varepsilon} = n + i\kappa$, which are the refractive index and the extinction coefficient, respectively. Finally, $\beta = \sqrt{2} |l(\varepsilon)| \Omega_0$ is the renormalized value of the bare Rabi frequency $\Omega_0 = dE/\hbar$, where d is the transition moment and E is the driving field amplitude. If the Lorentz local-field concept is implemented while performing summation or spatial integration in Eq. (1), then $\xi = (\pi c^3 / \omega_e^3) N_e \gamma_0$, where c is the speed of light. The factor $l(\varepsilon) = E_l / E_M$ is the ratio between the local- and Maxwellian-field amplitudes in the host so it could be derived as either $l = (\varepsilon + 2)/3$ or $l = 3\varepsilon / (2\varepsilon + 1)$ depending on the choice for the trick to get around the emitters during spatial integration. For the only emitter or when $N_e \rightarrow 0$ the terms with η^2 and ζ^2 disappear, no IOB is possible, and w becomes the standard component of the Bloch's vector \mathbf{B}_0 , i.e., $w_0 = (\Delta^2 + \Gamma^2) / (\Delta^2 + \Gamma^2 + \beta^2)$, which with $\varepsilon = 1$ takes the classic form.

The physical grounds of IOB may be explained by the plots (a) and (b) in Fig. 5. Plot (a) illustrates the comparison of the absorption contours that follow from v_0 and v for a fixed input power as functions of $\omega_e - \omega_0$. One can see that for certain frequencies of the driving force the absorption of a collective ensemble could be either abnormally low or high as compared to independent emitters. Thus, greater or smaller input power is required to create excitations for photoluminescence of a desired intensity. It is analogous to the classic picture of nonlinear oscillations as described, e.g., in [35]. Alternatively, plot (b) shows the acting field $\Omega \sim \Omega_0 + Au(\Omega_0)$ versus the input field Ω_0 , where A is a dimension factor that depends on how the local field is constructed. For moderate inputs the acting field is weakened by the response from the ensemble and fails to create the luminescing excitations efficiently. At stronger inputs the process responsible for building the response vanishes at some threshold point and the system makes a breakthrough to where $\Omega \sim \Omega_0$. Figure 5(c) shows the roots of Eq. (2) as functions of Ω_0 input. Since for a two-level system the total emission intensity must be $I \sim \gamma N_2$, where N_2 is the population of the excited state, we can plot the dimensionless function $I(\Omega_0) = (1/2)[1 - w(\Omega_0)]$. Substitution of w_0 gives the normal saturation curve while w solutions describe the S-shaped curve of IOB intensities. The branches w_1 and w_2 are the stable solutions and refer to the dim and the enhanced emission, respectively, while w_3 is unstable as could be shown via the standard analysis.

Now, let us look at how IOB may provide the flares. The S-shaped region has boundaries on the Ω_0 axis established by the threshold values Ω_0^{\downarrow} and Ω_0^{\uparrow} . The thresholds and the IOB width $\Omega_0^{\uparrow} - \Omega_0^{\downarrow}$ are sensitive to the parameters in Eq. (2). Note that in our theory every parameter, i.e., the cooperativity or the density of emitters, the detuning, and the relaxation rates,

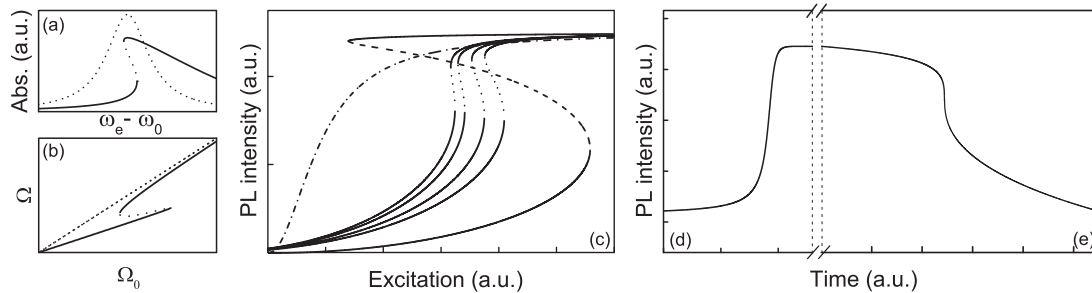


FIG. 5. (a) Absorption spectra of a single emitter (dotted line) and an IOB ensemble (solid line). (b) Effective Rabi versus bare Rabi frequencies. (c) A set of stable solutions for different values of dephasing rate (solid lines); unstable solutions (dashed segments). Dash-dotted lines show the normal Bloch solution. (d) Dim-to-enhanced transient. (e) Enhanced-to-dim transient. The linked (d) and (e) simulations show a variant of a typical time profile of a single superflare observed in the experiments (see Fig. 4 and the SM [13]).

appears to be formally dependent on the characteristics and the current state of the host medium. Thus we can assume they may be floating in real conditions and, therefore, make the steady states and the thresholds migrate as shown in Fig. 5. If our system, say, is tuned near Ω_0^\uparrow , later because of the migration (slow rising) Ω_0 input at some instant must leave the S-shaped region. This makes the system transmit to the bright state above (fast rising). The time evolution of this situation was simulated numerically and shown in Fig. 5(d). The simulations of the fast rising were performed by solving the equations of motion for $\mathbf{B}^T(t) = \{u(t), v(t), w(t)\}$ with the initial conditions $\mathbf{B}^T(0) = \{u_1(\Omega_0^\uparrow), v_1(\Omega_0^\uparrow), w_1(\Omega_0^\uparrow)\}$ and $\Omega_0 = \Omega_0^\uparrow + \delta\Omega$ where $\delta\Omega \ll \Omega_0^\uparrow$. It was established that the fast rising may last as long as dozens of thousands of excitation lifetimes. This is in agreement with the other IOB theories [30,36,37]. Once in the bright state the system may go back to dim emission in a similar way, i.e., by first falling slowly with the upper steady state and then breaking down having met the migrating threshold Ω_0^\downarrow . These processes were simulated and shown in Fig. 5(e).

The profiles and reoccurrence of the flares are subject to repeated weakly fluctuating parameters like γ_\perp (temperature) or N_e (quenching of few emitters) because of the changes in the host. Equation (2) provides returning to the enhanced state after excitation interruption which corresponds to the experimental observation shown in Fig. 4. Multiple steady states, a richer variety of instabilities, and extra paths for switchings are peculiar for multilevel systems as described in [38]. The four-level GeV scheme must be implemented in simulations as soon as the oscillator strengths have been measured and quantum efficiencies established. The hybrid ex-/intrinsic instabilities could be studied with Eq. (1) by adjusting the field parameters.

In conclusion, we have discovered experimentally the phenomenon of strong variations in photoluminescence intensity from single diamond microcrystal with GeV centers. This effect was detected for only one sample from the dozens

of microdiamonds observed. The flares appear stochastically under cw-laser excitation. Each flare looks like a lasting enhanced emission intensity with fast (seconds) rising, the steady state (up to dozens of seconds), and slow (dozens of seconds) decay. We suggest the model which qualitatively describes the temporal profiles of the flares and considers instabilities in an ensemble of emitters. The intrinsic mechanism lies in coupling between the emitters through the mean field while switchings occur because of changing parameters. The analysis has shown the following: (1) It is a very lucky occasion that all parameters appear such that they allow optical instabilities to occur. (2) The theory allows simulations of the temporal profiles by variation of the parameters while the core equation is flexible towards introducing new circumstances. (3) Short interruptions of the input do not bring the system to another steady state, as was seen in the experiment. (4) A multiple level scheme could be shown to demonstrate intrinsic multistability and provide the possibility for other intensities in the bright mode to be seen.

The discovered macroscopic phenomenon and theoretically supported understanding of its microscopic nature open a way for engineering photonic structures for applications in quantum optics and related areas.

This research was supported by the Russian Foundation for Basic Research (Grant No. 18-29-19200). E.A. Ekimov (synthesis, preparation and characterization of diamond samples, discussion of results) acknowledges support from the Russian Science Foundation (Grant No. 19-12-00407). The work on laser spectroscopy of particles is among the activities of the laboratory “Physics of the nanostructured materials” of the Moscow State Pedagogical University in collaboration with the Centre of collective usage “Structural diagnostics of materials” of the Federal Research Center RAS “Crystallography and photonics”, supported by the project of the Ministry of Science and Higher Education of the Russian Federation (AAAA-A20-120061890084-9).

[1] L. Mandel and E. Wolf, Optical coherence and quantum optics, *American Journal of Physics* (Cambridge University Press, Cambridge, UK, 1995), pp. 1192.

[2] F. Jelezko and J. Wrachtrup, Single defect centres in diamond: A review, *Phys. Status Solidi A* **203**, 3207 (2006).

- [3] B. Prasanna Venkatesh, M. L. Juan, and O. Romero-Isart, Cooperative Effects in Closely Packed Quantum Emitters with Collective Dephasing, *Phys. Rev. Lett.* **120**, 033602 (2018).
- [4] I. Aharonovich, A. D. Greentree, and S. Praver, Diamond photonics, *Nat. Photonics* **5**, 397 (2011).
- [5] G. Balasubramanian, P. Neumann, D. Twitchen, M. Markham, R. Kolesov, N. Mizuochi, J. Isoya, J. Achard, J. Beck, J. Tissler, V. Jacques, P. R. Hemmer, F. Jelezko, and J. Wrachtrup, Ultra-long spin coherence time in isotopically engineered diamond, *Nat. Mater.* **8**, 383 (2009).
- [6] T. Iwasaki, F. Ishibashi, Y. Miyamoto, Y. Doi, S. Kobayashi, T. Miyazaki, K. Tahara, K. D. Jahnke, L. J. Rogers, B. Naydenov, F. Jelezko, S. Yamasaki, S. Nagamachi, T. Inubushi, N. Mizuochi, and M. Hatano, Germanium-vacancy single color centers in diamond, *Sci. Rep.* **5**, 12882 (2015).
- [7] J.-W. Fan, I. Cojocaru, J. Becker, I. V. Fedotov, M. H. A. Alkahtani, A. Alajlan, S. Blakley, M. Rezaee, A. Lyamkina, Y. N. Palyanov, Y. M. Borzdov, Y.-P. Yang, A. Zheltikov, P. Hemmer, and A. V. Akimov, Germanium-vacancy color center in diamond as a temperature sensor, *ACS Photonics* **5**, 765 (2018).
- [8] M. H. Alkahtani, F. Alghannam, L. Jiang, A. Almethen, A. A. Rampersaud, R. Brick, C. L. Gomes, M. O. Scully, and P. R. Hemmer, Fluorescent nanodiamonds: past, present, and future, *Nanophotonics* **7**, 1423 (2018).
- [9] S. Häußler, G. Thiering, A. Dietrich, N. Waasem, T. Teraji, J. Isoya, T. Iwasaki, M. Hatano, F. Jelezko, A. Gali, and A. Kubanek, Photoluminescence excitation spectroscopy of SiV⁻ and GeV⁻ color center in diamond, *New J. Phys.* **19**, 063036 (2017).
- [10] S. Choi, V.N. Agafonov, V.A. Davydov, L.F. Kulikova, and T. Plakhotnik, Formation of interstitial silicon defects in Si- and Si,P-doped nanodiamonds and thermal susceptibilities of SiV⁻ photoluminescence band, *Nanotechnology* **31**, 205709 (2020).
- [11] M. K. Bhaskar, D. D. Sukachev, A. Sipahigil, R. E. Evans, M. J. Burek, C. T. Nguyen, L. J. Rogers, P. Siyushev, M. H. Metsch, H. Park, F. Jelezko, M. Lončar, and M. D. Lukin, Quantum Nonlinear Optics with a Germanium-Vacancy Color Center in a Nanoscale Diamond Waveguide, *Phys. Rev. Lett.* **118**, 223603 (2017).
- [12] E. A. Ekimov, S. G. Lyapin, K. N. Boldyrev, M. V. Kondrin, R. Khmel'nitskiy, V. A. Gavva, T. V. Kotereva, and M. N. Popova, Germanium-vacancy color center in isotopically enriched diamonds synthesized at high pressures, *JETP Lett.* **102**, 701 (2015).
- [13] See Supplemental Material at <http://link.aps.org/supplemental/10.1103/PhysRevB.102.060301> for sample preparation, initial materials and synthesis of the diamonds; descriptions of the experimental techniques and equipment; AFM images of the diamond microcrystals; temporal profiles of the PL flares; PLE spectra; analysis of PL intensity-falling curves; PL intensity versus cw-laser input power; derivation of IOB equations.
- [14] I. Y. Eremchev, M. Y. Eremchev, and A. V. Naumov, Multi-functional far-field luminescence nanoscope for studying single molecules and quantum dots, *Physics-Uspexhi* **62**, 294 (2019).
- [15] E. Ekimov, M. Kondrin, V. Krivobok, A. Khomich, I. Vlasov, R. Khmel'nitskiy, T. Iwasaki, and M. Hatano, Effect of Si, Ge and Sn dopant elements on structure and photoluminescence of nano- and microdiamonds synthesized from organic compounds, *Diam. Relat. Mater.* **93**, 75 (2019).
- [16] I. Y. Eremchev, Y. G. Vainer, A. V. Naumov, and L. Kador, Observation of structural relaxations in disordered solid media via spectral histories of single impurity molecules, *Phys. Solid State* **55**, 710 (2013).
- [17] I. Eremchev, I. S. Osad'ko, and A. V. Naumov, Auger ionization and tunneling neutralization of single CdSe/ZnS nanocrystals revealed by excitation intensity variation, *J. Phys. Chem. C* **120**, 22004 (2016).
- [18] R. M. Dickson, A. B. Cubitt, R. Y. Tsien, and W. E. Moerner, On/off blinking and switching behavior of single molecules of green fluorescent protein, *Nature (London)* **388**, 355 (1997).
- [19] M. Nirmal, B. O. Dabbousi, M. G. Bawendi, J. J. Macklin, J. K. Trautman, T. D. Harris, and L. E. Brus, Fluorescence intermittency in single cadmium selenide nanocrystals, *Nature (London)* **383**, 802 (1996).
- [20] Y. Tian, A. Merdasa, M. Peter, M. Abdellah, K. Zheng, C. S. Ponseca, T. Pullerits, A. Yartsev, V. Sundström, and I. G. Scheblykin, Giant photoluminescence blinking of perovskite nanocrystals reveals single-trap control of luminescence, *Nano Lett.* **15**, 1603 (2015).
- [21] N. Aslam, G. Waldherr, P. Neumann, F. Jelezko, and J. Wrachtrup, Photo-induced ionization dynamics of the nitrogen vacancy defect in diamond investigated by single-shot charge state detection, *New J. Phys.* **15**, 013064 (2013).
- [22] A. Halder, N. Pathoor, A. Chowdhury, and S. K. Sarkar, Photoluminescence flickering of micron-sized crystals of methylammonium lead bromide: Effect of ambience and light exposure, *J. Phys. Chem. C* **122**, 15133 (2018).
- [23] S. Feofilov and A. Kulinkin, Spontaneous temperature and fluorescence oscillations in CaS:Eu²⁺ crystals excited in the long-wavelength tail of the absorption spectrum, *J. Lumin.* **170**, 121 (2016).
- [24] H. M. Gibbs, S. L. McCall, and T. N. C. Venkatesan, Differential Gain and Bistability Using a Sodium-Filled Fabry-Perot Interferometer, *Phys. Rev. Lett.* **36**, 1135 (1976).
- [25] M. P. Hehlen, H. U. Güdel, Q. Shu, J. Rai, S. Rai, and S. C. Rand, Cooperative Bistability in Dense, Excited Atomic Systems, *Phys. Rev. Lett.* **73**, 1103 (1994).
- [26] P. Mandel and T. Erneux, Switching times in absorptive optical bistability, *Opt. Commun.* **42**, 362 (1982).
- [27] B. Segard, J. Zemmouri, and B. Macke, Switching delays in optical bistability: An experimental study, *Opt. Commun.* **60**, 323 (1986).
- [28] Y. Nishiyama, Long-time behavior of optical bistability, *Phys. Rev. A* **21**, 1618 (1980).
- [29] J. Bigot, A. Daunois, and P. Mandel, Slowing down far from the limit points in optical bistability, *Phys. Lett. A* **123**, 123 (1987).
- [30] B. S. Nugroho, A. A. Iskandar, V. A. Malyshev, and J. Knoester, Bistable optical response of a nanoparticle heterodimer: Mechanism, phase diagram, and switching time, *J. Chem. Phys.* **139**, 014303 (2013).
- [31] H. Zhang, G. Wang, D. Sun, X. Li, and H. Sun, Optical bistability and multistability induced by quantum coherence in diamond germanium-vacancy color centers, *Appl. Opt.* **58**, 2522 (2019).

- [32] I. V. Ryzhov, R. F. Malikov, A. V. Malyshev, and V. A. Malyshev, Nonlinear optical response of a two-dimensional quantum-dot supercrystal: Emerging multistability, periodic and aperiodic self-oscillations, chaos, and transient chaos, *Phys. Rev. A* **100**, 033820 (2019).
- [33] D. V. Kuznetsov, V. K. Roerich, and M. G. Gladush, Local field and radiative relaxation rate in a dielectric medium, *J. Exp. Theor. Phys.* **113**, 647 (2011).
- [34] D. V. Kuznetsov, V. K. Roerich, and M. G. Gladush, Using BBGKY hierarchies to study the effect of the local field on the rate of radiative relaxation of quantum systems in a dielectric medium, *Theor. Math. Phys.* **168**, 1078 (2011).
- [35] L. Landau and E. Lifshitz, *Mechanics*, 3rd ed. (Butterworth-Heinemann, Oxford, 1976), pp. 58–95.
- [36] E. C. Jarque and V. A. Malyshev, Nonlinear resonance reflection from and transmission through a dense glassy system built up of oriented linear Frenkel chains: Two-level model, *J. Chem. Phys.* **115**, 4275 (2001).
- [37] R. F. Malikov and V. A. Malyshev, Optical bistability and hysteresis of a thin layer of resonant emitters: Interplay of inhomogeneous broadening of the absorption line and the Lorentz local field, *Opt. Spectrosc.* **122**, 955 (2017).
- [38] R. A. Vlasov, A. M. Lemeza, and M. G. Gladush, Dynamical instabilities of spectroscopic transitions in dense resonant media, *Laser Phys. Lett.* **10**, 045401 (2013).